JBC RESEARCH ARTICLE

Metabolic flexibility maintains proliferation and migration of FGFR signaling–deficient lymphatic endothelial cells

Received for publication, July 21, 2021, and in revised form, August 24, 2021 Published, Papers in Press, August 30, 2021,
https://doi.org/10.1016/j.jbc.2021.101149

Hongyuan Song[1,‡], **Jie Zhu**[1,‡], **Ping Li**[1], **Fei Han**[1], **Longhou Fang**[2,3,4], **and Pengchun Yu**[1,5,*]

From the [1]*Cardiovascular Biology Research Program, Oklahoma Medical Research Foundation, Oklahoma City, Oklahoma, USA;* [2]*Department of Cardiovascular Sciences, Center for Cardiovascular Regeneration,* [3]*Department of Ophthalmology, Blanton Eye Institute, Houston Methodist Institute for Academic Medicine, Houston Methodist Research Institute, Houston, Texas, USA;* [4]*Department of Cardiothoracic Surgeries, Weill Cornell Medical College, Cornell University, New York City, New York, USA;* [5]*Department of Cell Biology, University of Oklahoma Health Sciences Center, Oklahoma City, Oklahoma, USA*

Edited by John Denu

Metabolic flexibility is the capacity of cells to alter fuel metabolism in response to changes in metabolic demand or nutrient availability. It is critical for maintaining cellular bioenergetics and is involved in the pathogenesis of cardiovascular disease and metabolic disorders. However, the regulation and function of metabolic flexibility in lymphatic endothelial cells (LECs) remain unclear. We have previously shown that glycolysis is the predominant metabolic pathway to generate ATP in LECs and that fibroblast growth factor receptor (FGFR) signaling controls lymphatic vessel formation by promoting glycolysis. Here, we found that chemical inhibition of FGFR activity or knockdown of FGFR1 induces substantial upregulation of fatty acid β-oxidation (FAO) while reducing glycolysis and cellular ATP generation in LECs. Interestingly, such compensatory elevation was not observed in glucose oxidation and glutamine oxidation. Mechanistic studies show that FGFR blockade promotes the expression of carnitine palmitoyltransferase 1A (CPT1A), a rate-limiting enzyme of FAO; this is achieved by dampened extracellular signal–regulated protein kinase activation, which in turn upregulates the expression of the peroxisome proliferator–activated receptor alpha. Metabolic analysis further demonstrates that CPT1A depletion decreases total cellular ATP levels in FGFR1-deficient rather than wildtype LECs. This result suggests that FAO, which makes a negligible contribution to cellular energy under normal conditions, can partially compensate for energy deficiency caused by FGFR inhibition. Consequently, CPT1A silencing potentiates the effect of FGFR1 knockdown on impeding LEC proliferation and migration. Collectively, our study identified a key role of metabolic flexibility in modulating the effect of FGFR signaling on LEC growth.

To maintain energy homeostasis, cells need to switch substrates for energy generation according to changes in metabolic demand or nutrient availability (1). This phenomenon, termed metabolic flexibility, was initially found in skeletal muscle, which can efficiently alter fuel preference in response to fasting and insulin infusions (2). In addition to skeletal muscle, metabolic flexibility also occurs in a few other tissues (*e.g.*, adipose tissue) and cell types (*e.g.*, pancreatic β-cells, cardiomyocytes) to help ensure proper cellular and physiological functions (3, 4). Notably, the impairment of metabolic flexibility is strongly associated with obesity, type 2 diabetes mellitus, and heart failure and impacts the pathophysiological processes underlying these diseases (1, 3, 5, 6).

Lymphatic endothelial cells (LECs) are building blocks of lymphatic vessels, which maintain tissue fluid homeostasis and act as essential conduits for trafficking of immune cells and tumor cells (7, 8). Excessive lymphangiogenesis (*i.e.*, lymphatic vessel formation) is involved in inflammatory disease and tumor metastasis, while insufficient lymphatic vessel growth may cause lymphedema, a medical condition that is characterized by swelling because of abnormal accumulation of interstitial fluid in tissues (9–11). Because of its importance, lymphangiogenesis has been extensively studied in order to identify novel strategies for treating diseases that are associated with lymphatic abnormalities.

Lymphangiogenesis, which involves active LEC proliferation and migration, is driven by growth factor signaling (12). Vascular endothelial growth factor C has been shown by numerous studies to play an indispensable role in this process through vascular endothelial growth factor receptors (13). In contrast, the role of fibroblast growth factor (FGF) signaling in lymphatic vessel formation is much less understood. The FGF family of growth factors is composed of 22 members, with FGF2 as a robust mitogen to stimulate lymphangiogenesis both *in vitro* and *in vivo* (14, 15). The effects of FGFs are mediated by four types of FGF receptors (FGFRs; FGFR1–FGFR4) (16). FGFR1 is the predominant FGFR in LECs, and knockdown of FGFR1 is sufficient to impair LEC proliferation, migration, and tube formation induced by FGF2 *in vitro* (15). However, during lymphatic vessel formation *in vivo*, the effect caused by loss of FGFR1 can be compensated by FGFR3, which is upregulated in LECs during lymphatic differentiation and is also required for lymphangiogenesis (17–19). As such, we found that while genetic deletion of *Fgfr1* in LECs has no impact, double knockout of both *Fgfr1* and *Fgfr3* leads to

‡ These authors contributed equally to this work.
* For correspondence: Pengchun Yu, Pengchun-Yu@omrf.org.

profound defects of lymphatic vascular development in mice (20). Collectively, these results demonstrate an important but complex role of FGFR signaling in lymphangiogenesis.

Recent advances have identified endothelial cell (EC) metabolism as a key process regulating lymphatic vessel formation (21–25). We and others found that glycolysis provides more than 70% of ATP in LECs (20, 26). Our studies further show that the effect of FGFR signaling on lymphangiogenesis is mediated by glycolysis (20). Knockdown of FGFR1—the most abundant member of the FGFR family—in LECs selectively reduces the expression of the glycolytic enzyme hexokinase 2 (HK2), and consequently suppresses glycolysis and ATP production, which are required for active angiogenic behavior of LECs (20). Functionally, lymphatic-specific deletion of *Hk2* in mice impairs lymphatic vascular development and abolishes the ability of FGF2 to promote lymphangiogenesis (20). In addition to glycolysis, fatty acid β-oxidation (FAO) also has been shown to play a critical role in lymphatic vessel formation (27). Carnitine palmitoyltransferase 1 (CPT1) is a group of rate-limiting enzymes of FAO, with CPT1A as the most abundant isoform in LECs (27). CPT1A depletion does not reduce ATP levels in ECs, suggesting that FAO makes a negligible contribution to endothelial energy production under normal conditions (28). Interestingly, CPT1A knockdown impairs endothelial proliferation by reducing the generation of acetyl-CoA, which can contribute to nucleotide synthesis for DNA replication (28). Recent studies further demonstrate that glutamine metabolism is crucial for EC proliferation and angiogenesis by maintaining tricarboxylic acid cycle anaplerosis, asparagine synthesis, and redox balance (29, 30). Despite the importance of glucose, glutamine, and fatty acids, how metabolism of these different substrates is coordinated to support LEC growth is unknown.

In our current study, we sought to determine the impact of FGFR signaling on utilization of glucose, glutamine, and fatty acids in LECs. During this process, we unexpectedly discovered a balance between glycolysis and FAO, which plays an important role in regulating FGFR-mediated energy generation and angiogenic behavior of cultured LECs.

Results

FGFR inhibition upregulates FAO while reducing glycolysis in LECs

To assess the potential impact of FGFR signaling on glucose oxidation, glutamine oxidation, and FAO, we treated proliferating human dermal LECs (HDLECs) with ASP5878, a highly specific FGFR inhibitor (31, 32), for 2 days. HDLECs were cultured in EC growth medium and kept at subconfluency throughout the experiments to maintain them in a proliferative state. At the end of ASP5878 treatment, we incorporated 5-^{3}H-glucose, 6-^{14}C-glucose, ^{14}C(U)-glutamine, 9,10-^{3}H-palmitic acid, or 1-^{14}C-oleic acid into the culture medium and calculated flux of glycolysis, glucose oxidation, glutamine oxidation, and FAO through the measurement of $^{3}H_2O$ or $^{14}CO_2$ generation. Consistent with our previous report (20), ASP5878 treatment drastically reduced glycolytic flux (Fig. 1*A*). FGFR inhibition also impaired glucose oxidation but did not affect glutamine oxidation (Fig. 1, *B* and *C*). In contrast, FAO in HDLECs was significantly enhanced after ASP5878 treatment (Fig. 1, *D* and *E*). To further confirm these observations that were generated with the FGFR chemical inhibitor, we transfected HDLECs with nontargeting or FGFR1-specific siRNA. Three days following siRNA transfection, we trypsinized control or FGFR1 siRNA-transfected HDLECs and replated them into new culture dishes to obtain subconfluent cells for analyses the next day. Western blotting showed that FGFR1 proteins were effectively depleted by siRNA treatment (Fig. 1, *F* and *G*). We further used 5-^{3}H-glucose, 9,10-^{3}H-palmitic acid, and 1-^{14}C-oleic acid to examine the effect of FGFR1 knockdown on flux of glycolysis and FAO. Our data showed that FGFR1 siRNA treatment significantly upregulated FAO while reducing glycolysis (Fig. 1, *H–J*). Together, our findings suggest the existence of a balance between glycolysis and FAO in LECs and reveal the importance of FGFR signaling in maintaining this balance.

FGFR blockade increases CPT1A expression for promoting FAO in LECs

Next, we sought to elucidate the molecular mechanism by which FGFR signaling inhibition enhanced FAO. Because CPT1A promotes FAO as a rate-limiting step in LECs and plays a critical role in lymphatic vessel formation (27), we examined whether FGFR activity regulates CPT1A expression. Treatment of HDLECs with ASP5878 for 2 days increased CPT1A protein levels while reducing the expression of HK2 (Fig. 2, *A–C*), which is consistent with our previous report (20). FGFR1 knockdown also led to reduction of HK2 and upregulation of CPT1A expression, albeit to a lesser extent than with the FGFR inhibitor (Fig. 2, *D–G*). We further confirmed these observations with a second siRNA, which targets a different region in *FGFR1* mRNA (Fig. S1, *A–C*). We then assessed whether CPT1A elevation was required for the effect of FGFR inhibition on FAO. Our data showed that depletion of CPT1A expression by siRNAs prevented ASP5878 or FGFR1 siRNA treatment from increasing FAO flux in HDLECs (Fig. 2, *H–J*). Collectively, our findings suggest that FGFR signaling regulates FAO by controlling CPT1A expression.

FAO inhibition enhances the effect of FGFR1 knockdown on suppressing energy generation, proliferation, and migration of LECs

We next explored the functional significance of FGFR inhibition–induced FAO upregulation for LECs. Previous studies show that FAO inhibition does not cause energy stress in ECs (27, 28). Consistently, we also found that CPT1A knockdown in HDLECs did not affect total ATP levels (Fig. 3*A*). However, CPT1A deficiency significantly potentiated the effect of FGFR1 siRNA on suppressing ATP production (Fig. 3*A*). We then examined the impact of FAO inhibition on LEC proliferation and migration, which are critically involved in lymphatic vessel formation. Our data demonstrated that although knockdown of CPT1A or FGFR1 alone reduced LEC

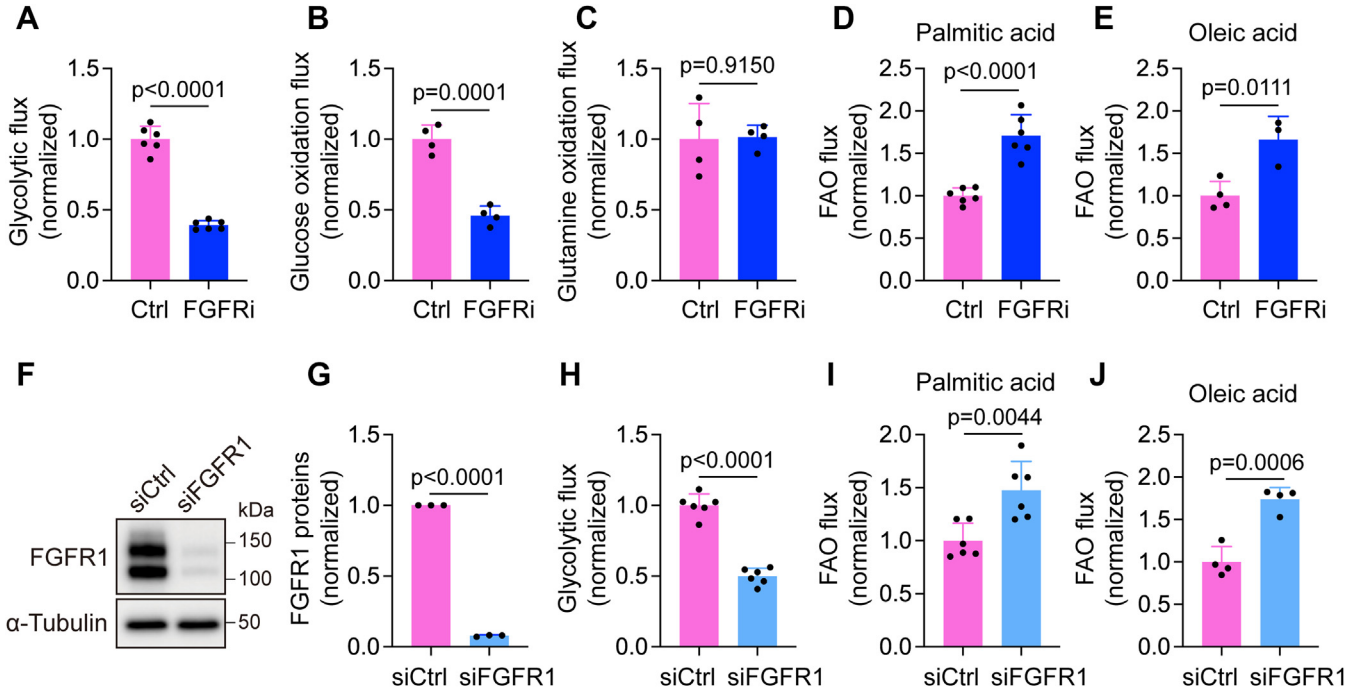

Figure 1. FGFR inhibition upregulates FAO while suppressing glycolysis in HDLECs. *A–E*, HDLECs were treated with vehicle or the FGFR inhibitor ASP5878 for 2 days and then analyzed for glycolytic flux with 5-^{3}H-glucose, glucose oxidation flux with 6-^{14}C-glucose, glutamine oxidation flux with ^{14}C(U)-glutamine, and FAO flux with 9,10-^{3}H-palmitic acid and 1-^{14}C-oleic acid (representative of two independent experiments). n = 6 biological replicates for (*A*), n = 4 biological replicates for (*B*), n = 4 biological replicates for (*C*), n = 6 biological replicates for (*D*), and n = 3 to 4 biological replicates for (*E*). *F* and *G*, Western blot analysis (*F*) and densitometric quantification (n = 3 independent experiments) (*G*) of FGFR1 proteins in HDLECs transfected with nontargeting (control) or FGFR1 siRNA. α-Tubulin served as a loading control. *H–J*, HDLECs transfected with nontargeting (control) or FGFR1 siRNA were analyzed for glycolytic flux with 5-^{3}H-glucose and for FAO flux with 9,10-^{3}H-palmitic acid and 1-^{14}C-oleic acid (representative of two independent experiments). n = 6 biological replicates for (*H*), n = 6 biological replicates for (*I*), and n = 4 biological replicates for (*J*). Data represent mean ± SD; *p* values were calculated by unpaired *t* test. FAO, fatty acid β-oxidation; FGFR, fibroblast growth factor receptor; HDLEC, human dermal lymphatic endothelial cell.

proliferation, their combined depletion resulted in more dramatic impairment (Fig. 3*B*). We further used an *in vitro* scratch assay to determine the role of FAO in LEC migration. We found that CPT1A knockdown did not affect migration in wildtype LECs (Fig. 3, *C* and *D*), which was consistent with a previous report (28). However, CPT1A depletion aggravated LEC migration defects caused by FGFR1 knockdown (Fig. 3, *C* and *D*).

Suppression of glycolysis per se *does not lead to upregulation of CPT1A expression in LECs*

To test whether CPT1A upregulation was secondary to an impairment of glycolysis caused by FGFR inhibition, we treated HDLECs with 2-deoxy-D-glucose (2DG), a potent inhibitor of glycolysis. Our data showed that 2DG failed to increase CPT1A levels (Fig. S2, *A* and *B*). These data suggest that FGFR signaling controls CPT1A expression independent of glycolysis.

FGFR1 depletion upregulates CPT1A expression in LECs through extracellular signal–regulated protein kinase signaling

One major pathway downstream of FGFR activation is RAF–MEK–extracellular signal–regulated protein kinase (ERK) signaling (33). Previous studies have shown that this pathway plays key roles in FGF-dependent control of angiogenesis and LEC differentiation (34, 35). Therefore, we sought to determine whether ERK signaling is involved in FGFR inhibition–induced CPT1A upregulation in LECs. We first examined ERK phosphorylation (Thr202/Tyr204) in HDLECs transfected with control or FGFR1 siRNA. We found that FGFR1 knockdown reduced levels of phosphorylated ERK while elevating CPT1A expression (Fig. 4*A* and Fig. S3*A*). Next, to investigate whether FGFR1 deficiency–caused CPT1A increase was due to impaired ERK signaling, we took advantage of RAF1^{S259A}, an RAF1 gain-of-function mutation that can activate ERK in ECs (36, 37). Consistent with the previous studies, transduction of HDLECs with a lentiviral vector expressing RAF1^{S259A} increased ERK phosphorylation (Fig. 4*B*). Importantly, we found that CPT1A levels were reduced concurrently with ERK activation in these cells (Fig. 4*B*). Moreover, RAF1^{S259A} expression was sufficient to normalize CPT1A expression in FGFR1 siRNA-transfected HDLECs (Fig. 4*C*). We also treated HDLECs with 20 μM of U0126, a highly specific MEK inhibitor, for 2 days. We found that inhibition of ERK activation led to CPT1A upregulation, similar to the effect of FGFR1 knockdown (Fig. 4, *D* and *E*). Collectively, these data suggest that FGFR-dependent regulation of CPT1A is mediated by ERK signaling.

To understand how FGFR–ERK signaling controls CPT1A expression, we performed quantitative PCR (qPCR) to examine *CPT1A* mRNA levels. Our data showed that FGFR inhibition by knocking down FGFR1 significantly increased *CPT1A*

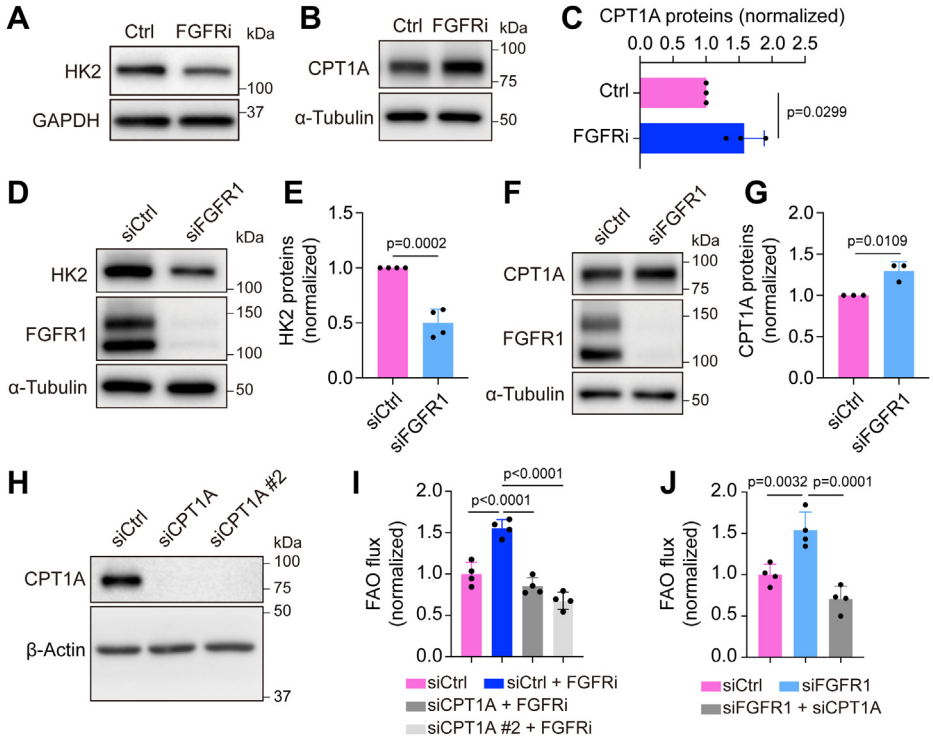

Figure 2. FGFR blockade increases CPT1A expression for promoting FAO in HDLECs. *A*, Western blot analysis of HK2 and GAPDH (loading control) in HDLECs treated with vehicle or the FGFR inhibitor ASP5878 for 2 days (representative of three independent experiments). *B* and *C*, Western blot analysis (*B*) and densitometric quantification (n = 3 independent experiments) (*C*) of CPT1A proteins in HDLECs treated with vehicle or the FGFR inhibitor ASP5878 for 2 days, nd α-tubulin served as a loading control. *D* and *E*, Western blot analysis (*D*) and densitometric quantification (n = 4 independent experiments) of HK2 proteins in HDLECs treated with nontargeting (control) or FGFR1 siRNA. *F* and *G*, Western blot analysis (*F*) and densitometric quantification (n = 3 independent experiments) (*G*) of CPT1A proteins in HDLECs treated with nontargeting (control) or FGFR1 siRNA. FGFR1 proteins were examined to confirm knockdown efficiency, and α-tubulin served as a loading control. *H*, Western blot analysis of CPT1A and α-tubulin (loading control) in HDLECs treated with nontargeting (control) or CPT1A siRNA (representative of two independent experiments). *I* and *J*, 9,10-^{3}H-palmitic acid–based measurement of FAO flux in HDLECs with the indicated treatments (n = 4 biological replicates). Note that CPT1A silencing normalized FAO flux increase caused by FGFR inhibition (*I*) or FGFR1 knockdown (*J*). Data represent mean ± SD; *p* values were calculated by unpaired *t* test (*C*, *E*, and *G*) or one-way ANOVA with Sidak's multiple comparisons test (*I* and *J*). CPT1A, carnitine palmitoyltransferase 1A; FAO, fatty acid β-oxidation; FGFR, fibroblast growth factor receptor; HDLEC, human dermal lymphatic endothelial cell; HK2, hexokinase 2.

mRNA (Fig. 4*F* and Fig. S3*B*). Moreover, FGFR1 depletion–induced *CPT1A* increase could be rescued by RAF1^{S259A} expression in HDLECs (Fig. 4*G*). Collectively, these results suggest that FGFR–ERK signaling regulates CPT1A expression at the transcriptional level.

FGFR–ERK signaling regulates CPT1A expression and FAO through the peroxisome proliferator–activated receptor alpha

Because our data suggest that FGFR–ERK signaling controls *CPT1A* transcription, we sought to identify transcriptional regulators that mediate this process. Peroxisome proliferator–activated receptors (PPARs) are a family of nuclear receptor proteins that regulate transcription of genes involved in a variety of cellular processes, including those involved in lipid metabolism (38). Recent studies have shown that PPARα and PPARγ, two PPAR isoforms, promote *CPT1A* transcription in hepatocytes and pulmonary arterial ECs, respectively (39, 40). These data led us to hypothesize that PPARα and PPARγ may mediate the effect of FGFR–ERK signaling on CPT1A expression. To test this idea, we first used GW6471, a well-characterized PPARα inhibitor (41, 42). We found that treatment of HDLECs with GW6471 suppressed CPT1A upregulation caused by the FGFR inhibitor ASP5878 (Fig. 5, *A* and *B*). Similarly, inhibition of PPARα also reduced FGFR1 knockdown–induced elevation of CPT1A expression in HDLECs (Fig. 5, *C* and *D*). To exclude potential nonspecific effects of GW6471, we confirmed these observations by using two different PPARα siRNAs. We found that PPARα knockdown in FGFR1-deficient HDLECs normalized CPT1A expression at both mRNA and protein levels (Fig. 5, *E* and *F* and Fig. S3*C*). Consistent with CPT1A expression, FAO increase caused by ASP5878 treatment or FGFR1 knockdown was also rescued by PPARα inhibition (Fig. 5, *G* and *H*). In contrast to PPARα, suppression of PPARγ by a specific inhibitor GW9662 (43, 44) failed to prevent FGFR blockade–induced upregulation of CPT1A (Fig. 5*I*). These data collectively suggest that PPARα, but not PPARγ, mediates FGFR-dependent regulation of CPT1A.

We further examined whether FGFR signaling controls PPARα. We found that FGFR1 knockdown significantly increased mRNA levels of *PPARA*, which encodes PPARα (Fig. 5*J* and Fig. S3*D*). Moreover, FGFR1 depletion–induced *PPARA* upregulation could be normalized by RAF1^{S259A} expression in HDLECs (Fig. 5*K*), indicating that PPARα functions downstream of ERK activation. Taken together, our data suggest that FGFR–ERK signaling regulates CPT1A expression and FAO in LECs through PPARα.

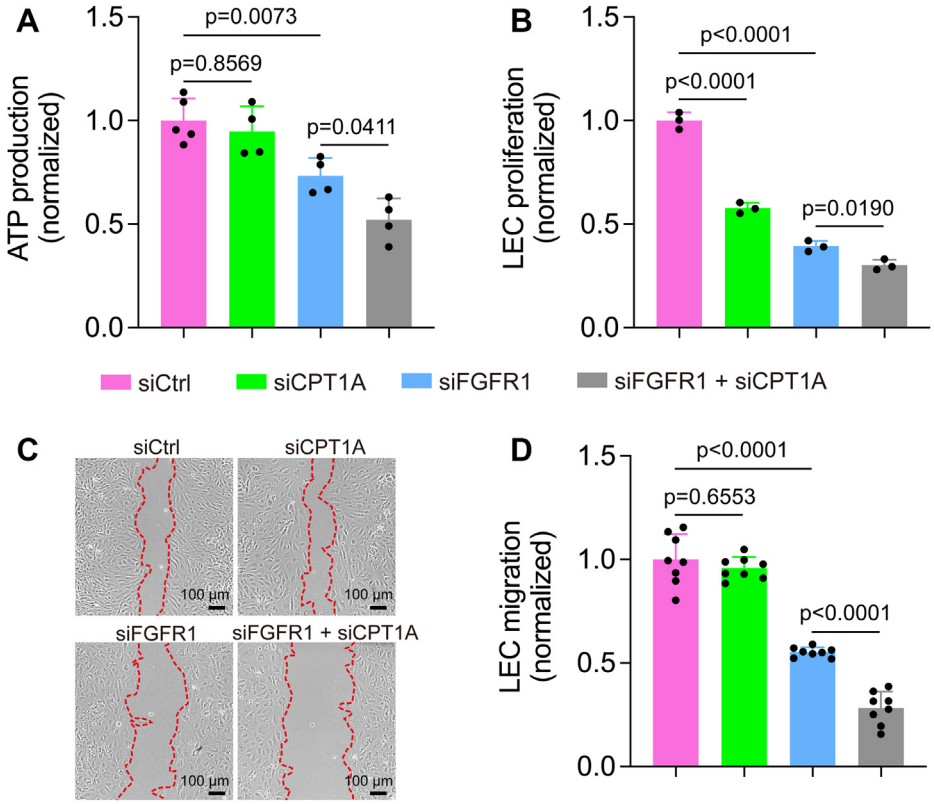

Figure 3. FAO inhibition potentiates the impact of FGFR1 knockdown on suppressing ATP generation, proliferation, and migration of HDLECs. *A*, ATP levels of HDLECs transfected with nontargeting (control) siRNA, CPT1A siRNA, FGFR1 siRNA, or a combination of both CPT1A and FGFR1 siRNAs (n = 4–5 technical replicates; representative of three independent experiments). *B*, proliferation of HDLECs transfected with nontargeting (control) siRNA, CPT1A siRNA, FGFR1 siRNA, or a combination of both CPT1A and FGFR1 siRNAs (n = 3 technical replicates; representative of three independent experiments). *C* and *D*, representative images (*C*) and quantification (*D*) of a wound-healing assay to assess the migration of HDLECs transfected with nontargeting (control) siRNA, CPT1A siRNA, FGFR1 siRNA, or a combination of both CPT1A and FGFR1 siRNAs (n = 8 imaging fields; representative of two independent experiments). *Red dotted lines* outline wound area at the last time points. Data represent mean ± SD; *p* values were calculated by one-way ANOVA with Sidak's multiple comparisons test. CPT1A, carnitine palmitoyltransferase 1A; FAO, fatty acid β-oxidation; FGFR1, fibroblast growth factor receptor 1; HDLEC, human dermal lymphatic endothelial cell.

Discussion

In the current study, we discovered that a balance between glycolysis and FAO exists in LECs and plays an important role in FGFR-mediated energy generation, LEC proliferation, and migration. While FGFR inhibition impairs glycolysis by reducing HK2 expression, it enhances FAO by upregulating CPT1A expression through ERK–PPARα signaling (Fig. 6). Such metabolic flexibility allows FAO to partially compensate for energy deficiency caused by FGFR1 knockdown. Functionally, suppression of FAO can exacerbate impaired LEC proliferation and migration caused by FGFR1 depletion. Our findings are reminiscent of the AMP-activated protein kinase (AMPK), which is an extensively studied energy sensor linking glycolysis with FAO. Energy stress because of defective glycolysis activates AMPK, which in turn enhances CPT1 activity and FAO by reducing the generation of a CPT1 inhibitor, malonyl-CoA (45). However, we found that glycolytic inhibition caused by 2DG treatment, which activates AMPK in ECs (46), does not increase CPT1A levels (Fig. S2), indicating that FGFR-mediated regulation of CPT1A expression is independent of AMPK. Therefore, our study reveals a new mechanism (promoting CPT1A expression) that functions in parallel with AMPK (enhancing CPT1 activity). These two mechanisms might collectively contribute to FGFR inhibition–induced FAO upregulation. Our results are also consistent with a recent study, which shows that compared with blood ECs (BECs) in the proliferative state, quiescent BECs, which were obtained through contact inhibition or activating Notch signaling, reduce glycolytic flux but potentiate FAO by increasing CPT1A (47). In turn, the higher level of FAO sustains redox homeostasis but does not support energy production in quiescent BECs (47). However, the mechanism through which CPT1A is induced in quiescent BECs remains to be determined.

Previous studies show that glycolysis generates most ATP in ECs, whereas FAO makes a negligible contribution (20, 26). Consistently, CPT1A knockdown in ECs does not impair ATP production and migration, which is a highly energy-demanding process (28). Although we obtained similar results in wildtype LECs, our data showed that CPT1A silencing decreases ATP levels and migration in FGFR1-deficient LECs (Fig. 3, *A*, *C*, and *D*), suggesting that FGFR suppression makes LECs rely on FAO for acquiring energy. FAO has been demonstrated to regulate EC proliferation by contributing carbons for nucleotide synthesis (27, 28). As such, we found that knockdown of CPT1A is sufficient to impede LEC

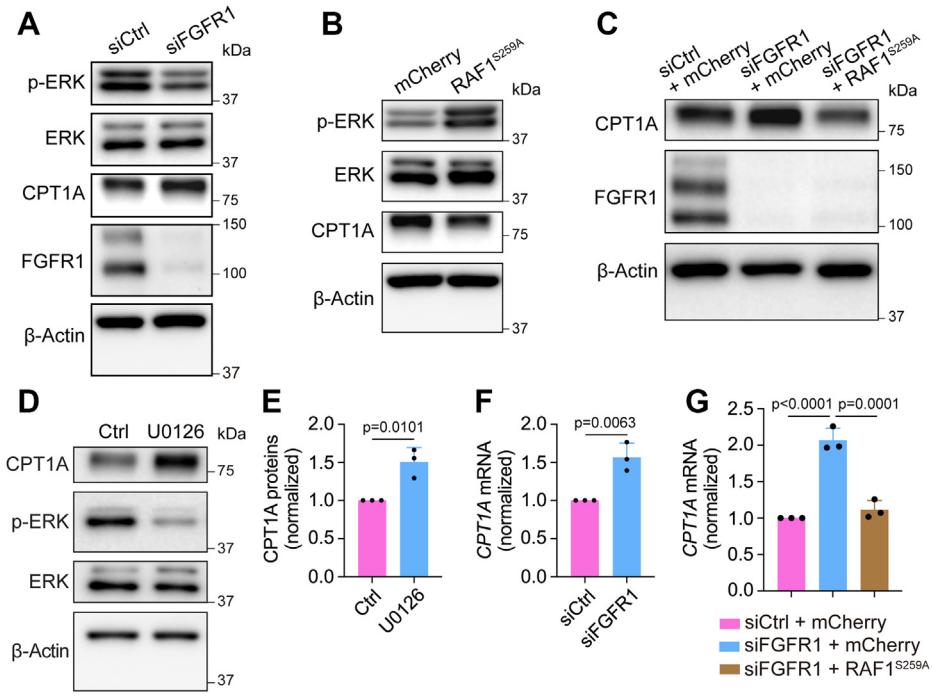

Figure 4. FGFR1 deficiency upregulates CPT1A expression in LECs through ERK signaling. *A*, Western blot analysis of phosphorylated ERK1/2 (Thr202/Tyr204), total ERK1/2, CPT1A, FGFR1, and β-actin (loading control) in HDLECs treated with nontargeting (control) or FGFR1 siRNA (representative of three independent experiments). *B*, Western blot analysis of phosphorylated ERK1/2 (Thr202/Tyr204), total ERK1/2, CPT1A, and β-actin (loading control) in HDLECs transduced with lentiviral vectors encoding mCherry or $RAF1^{S259A}$ (representative of three independent experiments). *C*, Western blot analysis of CPT1A, FGFR1, and β-actin (loading control) in HDLECs under the indicated conditions (representative of three independent experiments). Note that while FGFR1 knockdown promoted CPT1A expression, this effect was rescued by lentivirus-mediated expression of $RAF1^{S259A}$. *D* and *E*, Western blot analysis (*D*) and densitometric quantification (n = 3 independent experiments) (*E*) of CPT1A proteins in HDLECs treated with vehicle or the MEK inhibitor U0126 for 2 days, and β-actin served as a loading control. *F*, quantitative PCR analysis of *CPT1A* mRNA in HDLECs transfected with nontargeting (control) or FGFR1 siRNA (n = 3 independent experiments). *G*, quantitative PCR analysis of *CPT1A* mRNA in HDLECs showing that lentivirus-mediated expression of $RAF1^{S259A}$ normalized FGFR1 knockdown-induced upregulation of *CPT1A* mRNA (n = 3 independent experiments). Data represent mean ± SD; *p* values were calculated by unpaired *t* test (*E* and *F*) or one-way ANOVA with Sidak's multiple comparisons test (*G*). CPT1A, carnitine palmitoyltransferase 1A; ERK, extracellular signal–regulated protein kinase; FGFR1, fibroblast growth factor receptor 1; LEC, lymphatic endothelial cell.

proliferation, but depletion of both CPT1A and FGFR1 caused a more dramatic effect (Fig. 3*B*), which likely reflects the outcome of dual inhibition of ATP generation and nucleotide synthesis.

Our data show that ERK activation by $RAF1^{S259A}$ expression can normalize PPARα and CPT1A expression in LECs with FGFR inhibition (Figs. 4, *C* and *G* and 5*K* and Fig. S3*C*), suggesting that ERK mediates the effect of FGFRs on PPARα and CPT1A expression. These observations are consistent with previous studies on tumor and liver metabolism. For example, using the BRAF inhibitor PLX to suppress mitogen-activated protein kinase in $BRAF^{V600E}$-driven melanoma upregulates *PPARA* and *CPT1A* mRNA (48). In the mouse liver, ERK activation by expressing a constitutively active MEK reduces mRNA levels of *Ppara* and *Cpt1b* (49). However, ERK plays an opposite role in this process in livers of leptin receptor-deficient (*db/db*) mice: ERK activation increases, whereas ERK inhibition reduces *Ppara* and *Cpt1a* mRNA levels (50). These results indicate that the mechanisms by which ERK controls PPARα and CPT1 vary in different biological contexts.

FGFR inhibitors are actively tested in clinical trials to treat various types of tumors (51). Our previous work also demonstrates that chemical inhibition of FGFR activity reduces tumor lymphangiogenesis (20), which is critical for tumor metastasis (52). Given our findings in the current study, targeting both FGFR signaling and FAO may offer a more effective means of suppressing the formation of tumor-associated lymphatic vessels and therefore may improve current cancer therapies that use FGFR inhibitors.

Experimental procedures

Cell culture and transfection

HDLECs (HMVEC-dLyNeo-Der Lym Endo EGM-2MV) were purchased from Lonza and cultured in EBM2 basal medium with EGM-2 MV BulletKit. HDLECs were tested negative for *mycoplasma* by Lonza. Culture medium was changed every other day. Tissue culture plates were coated with 0.1% gelatin (Sigma) for 30 min at 37 °C and washed with Dulbecco's phosphate-buffered saline (Life Technologies) before cell plating. FGFR1 siRNA (Dharmacon; SMARTpool siRNAs with four target sequences: GCCACACUCUGCACCGCUA, CCACAGAAUUGGAGGCUAC, CAAAUGCCCUUCCAGUGGG, and GAAAUUGCAUGCAGUGCCG), FGFR1 siRNA #2 (Qiagen; target sequence: CAGAGATTTACCCATCGGGTA), CPT1A siRNA (Qiagen; target sequence: CTGGATGGGTATGGTCAAGAT), CPT1A siRNA #2 (Qiagen; target sequence: AACGATGTACGCCAAGATCGA), PPARα siRNA (Qiagen; target sequence: CAAGAGAATCTACGAGGCCTA), PPARα siRNA #2 (Qiagen; target sequence: AAGCTTTGGCTTTACGGAATA), and

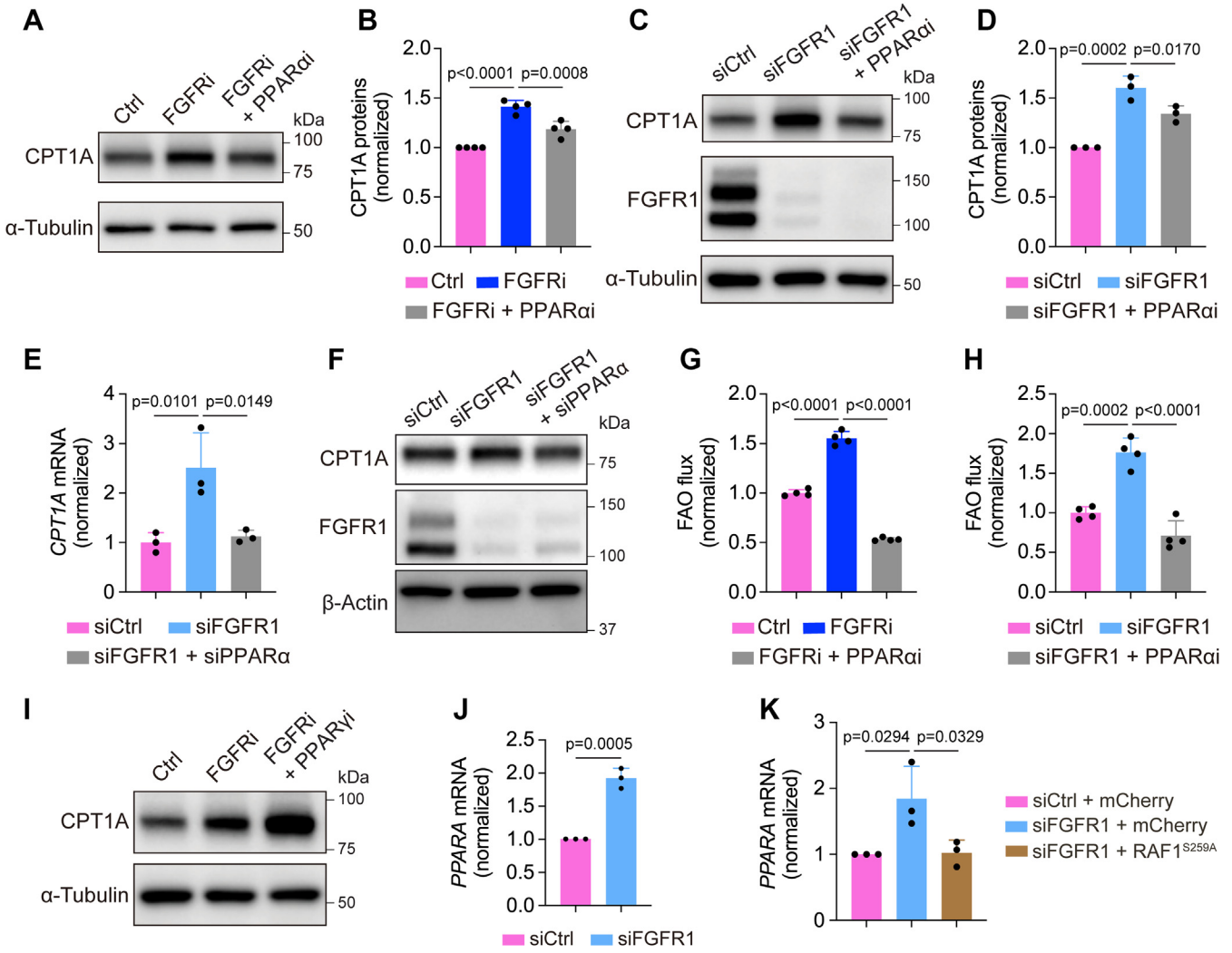

Figure 5. FGFR–ERK signaling regulates CPT1A expression and FAO through PPARα. *A* and *B*, Western blot analysis (*A*) and densitometric quantification (n = 4 biological replicates from three independent experiments) (*B*) of CPT1A proteins in HDLECs treated with vehicle, the FGFR inhibitor ASP5878, or a combination of ASP5878 and the PPARα antagonist GW6471. α-Tubulin served as a loading control. *C* and *D*, Western blot analysis (*C*) and densitometric quantification (n = 3 replicates from two independent experiments) (*D*) of CPT1A proteins in HDLECs treated with nontargeting (control) siRNA, FGFR1 siRNA, or both FGFR1 siRNA and the PPARα inhibitor GW6471. α-Tubulin was examined as a loading control. *E* and *F*, quantitative PCR (qPCR) analysis (n = 3 technical replicates; representative of two independent experiments) (*E*) and Western blotting (representative of two independent experiments) (*F*) of CPT1A expression in HDLECs transfected nontargeting (control) siRNA, FGFR1 siRNA, or a combination of FGFR1 siRNA and PPARα siRNA. β-actin was examined as a loading control. *G*, 9,10-^{3}H-palmitic acid–based measurement of FAO flux in HDLECs treated with vehicle, the FGFR inhibitor ASP5878, or a combination of ASP5878 and the PPARα antagonist GW6471 (n = 4 biological replicates; representative of two independent experiments). *H*, 9,10-^{3}H-palmitic acid–based measurement of FAO flux in HDLECs treated with nontargeting (control) siRNA, FGFR1 siRNA, or both FGFR1 siRNA and the PPARα inhibitor GW6471 (n = 4 biological replicates). *I*, Western blot analysis of CPT1A proteins in HDLECs treated with vehicle, the FGFR inhibitor ASP5878, or both ASP5878 and the PPARγ antagonist GW9662 (representative of three independent experiments). α-Tubulin served as a loading control. *J*, qPCR analysis of *PPARA* mRNA (encoding PPARα) in HDLECs transfected with nontargeting (control) or FGFR1 siRNA (n = 3 independent experiments). *K*, qPCR analysis of *PPARA* mRNA in HDLECs showing that lentivirus-mediated expression of RAF1^{S259A}-normalized FGFR1 knockdown-induced upregulation of *PPARA* mRNA (n = 3 independent experiments). Data represent mean ± SD; *p* values were calculated by unpaired *t* test (*J*) or one-way ANOVA with Sidak's multiple comparisons test (*B*, *D*, *E*, *G*, *H*, and *K*). CPT1A, carnitine palmitoyltransferase 1A; ERK, extracellular signal–regulated protein kinase; FAO, fatty acid β-oxidation; FGFR, fibroblast growth factor receptor; HDLEC, human dermal lymphatic endothelial cell; PPARα, peroxisome proliferator–activated receptor alpha.

nontargeting siRNA were commercially purchased and transfected by Lipofectamine RNAiMAX (Life Technologies). To assess the effect of FGFR1, CPT1A, and/or PPARα knockdown on metabolic processes and protein expression, HDLECs, transfected with relevant siRNA 2 or 3 days in advance, were replated and collected for indicated analysis approximately 16 h later when the cell confluency reached ∼80%. To assay the effect of PPARα inhibitor on FAO and protein expression after FGFR1 knockdown, HDLECs were transfected with indicated siRNAs 2 days in advance and then treated with GW6471 (10 μM) or GW9662 (20 μM) for another 2 days. HDLECs were treated with ASP5878 (200–400 nM) for 2 days and then assayed the resulting effect on metabolic processes and protein expression. To assay the effect of GW6471 and ASP5878 on FAO and CPT1A expression, HDLECs were treated with both ASP5878 and GW6471 for 2 days before the analyses.

Reagents

The FGFR inhibitor ASP5878 was purchased from Selleckchem (#S6539). The PPARα antagonist GW6471 was

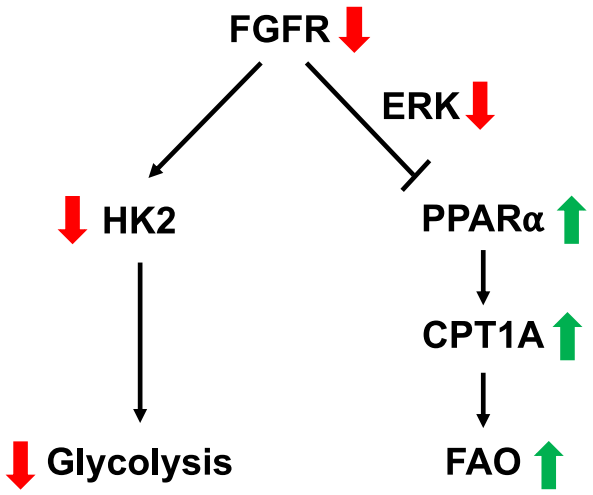

Figure 6. Schematic of the balance between glycolysis and FAO in LECs. In LECs, FGFR signaling promotes glycolysis while repressing FAO. When FGFR activity is inhibited, glycolysis is suppressed, resulting in reduction of ATP levels in LECs. In the meantime, FGFR-deficient LECs, through dampened ERK signaling, upregulate PPARα and CPT1A expression, consequently enhancing FAO. Upregulated FAO can partially compensate for energy deficiency caused by FGFR inhibition. CPT1A, carnitine palmitoyltransferase 1A; ERK, extracellular signal–regulated protein kinase; FAO, fatty acid β-oxidation; FGFR, fibroblast growth factor receptor; LEC, lymphatic endothelial cell; PPARα, peroxisome proliferator–activated receptor alpha.

purchased from Cayman Chemical (#11697). The PPARγ antagonist GW9662 was purchased from Sigma (#M6191). 2-DG was ordered from Sigma (#D8375). The MEK inhibitor U0126 was purchased from Sigma (#U120). Luminescence ATP detection assay system (ATPlite) was purchased from PerkinElmer. For Western blot analysis, the following antibodies were used: HK2 (Cell Signaling Technology; #2867, 1:1000), FGFR1 (Cell Signaling Technology; #9740, 1:1000), phospho-ERK (Cell Signaling Technology; #4370, 1:1000), ERK1/2 (Cell Signaling Technology; #4695, 1:2000), CPT1A (Abcam; #128568, 1:5000), GAPDH (Cell Signaling Technology, #5174; 1:5000), α-tubulin (Cell Signaling Technology, #2144; 1:5000), β-actin (Sigma, #A5316; 1:10,000). ImageJ (NIH) was used for densitometry quantification of Western blot bands.

Lentivirus generation

Lentiviral transfer plasmids encoding CMV promoter-driven RAF1^{S259A} (available at addgene) or mCherry (pLVX-mCherry-N1) were cotransfected with psPAX2 and VSV-G into 293T cells. Virus-containing media were collected 1 or 2 days after transfection and used to infect HDLECs in the presence of polybrene (2–4 μg/ml).

Measurement of glycolysis with [5-^{3}H]-glucose

Glycolytic flux was measured as previously described (53). Briefly, subconfluent HDLECs cultured in 12-well plates were incubated with 1 ml per well EBM2 medium (containing appropriate amounts of serum and supplement) with [5-^{3}H]-glucose (PerkinElmer) for 2 to 3 h. Then 0.8 ml per well medium was transferred into glass vials with hanging wells and filter papers soaked with water. After incubation in a cell culture incubator for at least 2 days to reach saturation, filter papers were taken out and the amount of evaporated ^3H_2O was measured in a scintillation counter.

Measurement of FAO with [9,10-^{3}H]-palmitic acid

FAO flux was measured using [9,10-^{3}H]-palmitic acid essentially as reported (53). Briefly, subconfluent HDLECs cultured in 12-well plates were incubated with 1 ml per well EBM2 medium (containing appropriate amounts of fatty acid–free bovine serum albumin, carnitine, and cold palmitic acid) with [9,10-^{3}H]-palmitic acid (PerkinElmer) for 6 h. Then, 0.8 ml per well medium was transferred into glass vials with hanging wells and filter papers soaked with water. After incubation in a cell culture incubator for at least 2 days to reach saturation, filter papers were taken out, and the amount of evaporated ^3H_2O was measured in a scintillation counter.

Measurement of FAO with [1-^{14}C]-oleic acid

FAO flux was measured using [1-^{14}C]-oleic acid as reported (54). Briefly, subconfluent HDLECs cultured in 12-well plates were incubated with 1 ml per well EBM2 medium (containing appropriate amounts of fatty acid–free bovine serum albumin and carnitine) with [1-^{14}C]-oleic acid (PerkinElmer) for 6 h. Then, the cells were lysed using 12% perchloric acid (Sigma–Aldrich; #244252), and the wells were covered immediately using filter papers soaked with hyamine hydroxide (PerkinElmer). After incubation in a fume hood for at least 12 h to reach saturation, filter papers were taken out, and the amount of evaporated $^{14}CO_2$ was measured in a scintillation counter.

Measurement of glucose oxidation with [6-^{14}C]-glucose

Glucose oxidation flux was measured as previously described (53). Briefly, subconfluent HDLECs cultured in 12-well plates were incubated with 1 ml per well EBM2 medium (containing appropriate amounts of serum and supplement) with [6-^{14}C]-glucose (PerkinElmer) for 6 h. Then, the cells were lysed using 12% perchloric acid, and the wells were covered immediately using filter papers soaked with hyamine hydroxide (PerkinElmer). After incubation in a fume hood for at least 12 h to reach saturation, filter papers were taken out, and the amount of evaporated $^{14}CO_2$ was measured in a scintillation counter.

Measurement of glutamine oxidation with [^{14}C(U)]-glutamine

Glutamine oxidation flux was measured as previously described (53). Briefly, subconfluent HDLECs cultured in 6-well plates were incubated with 2 ml per well EBM2 medium (containing appropriate amounts of serum and supplement) with [^{14}C(U)]-glutamine (PerkinElmer) for 6 h. Then, the cells were lysed using 12% perchloric acid, and the wells were covered immediately using filter papers soaked with hyamine hydroxide (PerkinElmer). After incubation in a fume hood for at least 12 h to reach saturation, filter papers were taken out, and the amount of evaporated $^{14}CO_2$ was measured in a scintillation counter.

Western blotting

Cells were lysed using radioimmunoprecipitation buffer, and protein concentrations were measured using the bicinchoninic acid assay. Proteins were first loaded and separated by SDS-PAGE and then transferred to a polyvinylidene difluoride membrane. The membrane was blocked with 5% nonfat milk for 45 min at room temperature and then incubated with relevant primary antibodies overnight at 4°. After incubating with horseradish peroxidase–conjugated secondary antibodies, the membrane was visualized with the SuperSignal West Pico PLUS Chemiluminescent Substrate (Thermo Fisher Scientific) using the ChemiDoc MP imaging system (Bio-Rad).

Cell proliferation

About 80,000 HDLECs were seeded into each well of a 6-well plate and incubated overnight. Cells were transfected with control, FGFR1, CPT1A, or combined FGFR and CPT1A siRNA and cultured for 4 days. Then, cell numbers were counted using a hemocytometer (Hausser Scientific Horsham).

ATP production

ATP levels were measured according to the manufacturer's instruction (PerkinElmer; 6016943). Briefly, HDLECs, which were transfected with control, FGFR1, CPT1A, or combined FGFR and CPT1A siRNA 3 days in advance, were replated to a 96-well plate, and ATP production analysis was performed approximately 12 h later. About 50 μl of mammalian cell lysis solution was added to each well, and the plate was shaken for 5 min at 700 rpm. Then, 50 μl of the substrate solution was added to the cells, and the plate was shaken for another 5 min at 700 rpm. After adapting the plate for 10 min, the luminescence was measured using FLUOstar Omega (BMG LABTECH).

Wound-healing migration assay

HDLEC migration was measured in a wound-healing assay, which used ibidi Culture-Inserts (ibidi) to generate the wound. An ibidi Culture-Insert has dimensions 9 × 9 × 5 mm (width × length × height) and is composed of two wells. One or two inserts were placed into one well of 6-well plates. HDLECs, which were transfected with control, FGFR1, CPT1A, or combined FGFR and CPT1A siRNA 3 days in advance, were replated to the wells of the inserts. When cells became fully confluent after attachment, Culture-Inserts were carefully removed by sterile tweezers to start cell migration. For studying the effect of FGFR1 and CPT1A siRNA on migration, the wound-healing process was monitored for approximately 11 h. A Nikon ECLIPSE Ti microscope with an ANDOR camera was used to image cells at the first time point (T_0) and the last time point ($T_{\text{end point}}$). For data analysis, ImageJ was used to measure the wound area at T_0 and $T_{\text{end point}}$. Migration area was obtained by subtracting area at $T_{\text{end point}}$ from area at T_0.

qPCR analysis

Total RNA was extracted from HDLECs using the TRIzol reagent (Thermo Fisher Scientific) or the RNeasy Plus Mini Kit (Qiagen) according to the manufacturer's instructions. The concentrations and quality of RNA were analyzed by Nanophotometer (IMPLEN). Complementary DNA synthesis was performed using the iScript cDNA synthesis kit (Bio-Rad). qPCR was performed with EvaGreen qPCR Master Mix (Bullseye) using the CFX96 Real-Time system (Bio-Rad).

Statistical analysis

Data represent mean ± SD. The number of biological and technical replicates and independent experiments is indicated in the legends to the figures. Statistical significance between two groups was determined by two-tailed unpaired t test, and statistical significance between multiple groups was calculated using one-way ANOVA with Sidak's multiple comparisons test. p Values are reported to four decimal places. Difference between experimental groups is considered statistically significant if $p < 0.05$.

Data availability

All data are contained in the article.

Supporting information—This article contains supporting information.

Acknowledgments—We thank Ms Summer Simeroth for proofreading the article and Drs Courtney Griffin, Sathish Srinivasan, Holly Van Remmen, and Chi Fung Lee for helpful discussions.

Author contributions—P. Y. conceptualization; H. S., J. Z., P. L., and F. H. methodology; H. S., J. Z., P. L., and F. H. formal analysis; H. S., J. Z., P. L., and F. H. investigation; L. F. resources; H. S. and P. Y. writing–original draft; H. S., J. Z., L. F., and P. Y. writing–review and editing; P. Y. supervision; P. Y. funding acquisition.

Funding and additional information—This project was supported by the American Heart Association 16BGIA27790081 and Internal Restorative Medicine to L. F. This work was also supported by the American Heart Association 19CDA34760260, grants from the Oklahoma Center for Adult Stem Cell Research and the Presbyterian Health Foundation, and Oklahoma Medical Research Foundation startup funding to P. Y.

Conflict of interest—The authors declare that they have no conflicts of interest with the contents of this article.

Abbreviations—The abbreviations used are: 2DG, 2-deoxy-D-glucose; AMPK, AMP-activated protein kinase; BEC, blood EC; CPT1A, carnitine palmitoyltransferase 1A; EC, endothelial cell; ERK, extracellular signal–regulated protein kinase; FAO, fatty acid β-oxidation; FGF, fibroblast growth factor; FGFR, fibroblast growth factor receptor; HDLEC, human dermal LEC; HK2, hexokinase 2; LEC, lymphatic endothelial cell; PPAR, peroxisome proliferator–activated receptor; qPCR, quantitative PCR.

References

1. Goodpaster, B. H., and Sparks, L. M. (2017) Metabolic flexibility in health and disease. *Cell Metab.* **25**, 1027–1036

2. Kelley, D. E., Goodpaster, B., Wing, R. R., and Simoneau, J. A. (1999) Skeletal muscle fatty acid metabolism in association with insulin resistance, obesity, and weight loss. *Am. J. Physiol.* **277**, E1130–E1141
3. Smith, R. L., Soeters, M. R., Wust, R. C. I., and Houtkooper, R. H. (2018) Metabolic flexibility as an adaptation to energy resources and requirements in health and disease. *Endocr. Rev.* **39**, 489–517
4. Oleson, B. J., Broniowska, K. A., Yeo, C. T., Flancher, M., Naatz, A., Hogg, N., Tarakanova, V. L., and Corbett, J. A. (2019) The role of metabolic flexibility in the regulation of the DNA damage response by nitric oxide. *Mol. Cell. Biol.* **39**, e00153-19
5. Muoio, D. M. (2014) Metabolic inflexibility: When mitochondrial indecision leads to metabolic gridlock. *Cell* **159**, 1253–1262
6. Vallerie, S. N., and Bornfeldt, K. E. (2015) Metabolic flexibility and dysfunction in cardiovascular cells. *Arterioscler. Thromb. Vasc. Biol.* **35**, e37–e42
7. Adams, R. H., and Alitalo, K. (2007) Molecular regulation of angiogenesis and lymphangiogenesis. *Nat. Rev. Mol. Cell Biol.* **8**, 464–478
8. Tammela, T., and Alitalo, K. (2010) Lymphangiogenesis: Molecular mechanisms and future promise. *Cell* **140**, 460–476
9. Karpanen, T., and Alitalo, K. (2008) Molecular biology and pathology of lymphangiogenesis. *Annu. Rev. Pathol.* **3**, 367–397
10. Oliver, G., and Srinivasan, R. S. (2008) Lymphatic vasculature development: Current concepts. *Ann. N. Y. Acad. Sci.* **1131**, 75–81
11. Alitalo, K. (2011) The lymphatic vasculature in disease. *Nat. Med.* **17**, 1371–1380
12. Alitalo, K., Tammela, T., and Petrova, T. V. (2005) Lymphangiogenesis in development and human disease. *Nature* **438**, 946–953
13. Vaahtomeri, K., Karaman, S., Makinen, T., and Alitalo, K. (2017) Lymphangiogenesis guidance by paracrine and pericellular factors. *Genes Dev.* **31**, 1615–1634
14. Cao, R., Ji, H., Feng, N., Zhang, Y., Yang, X., Andersson, P., Sun, Y., Tritsaris, K., Hansen, A. J., Dissing, S., and Cao, Y. (2012) Collaborative interplay between FGF-2 and VEGF-C promotes lymphangiogenesis and metastasis. *Proc. Natl. Acad. Sci. U. S. A.* **109**, 15894–15899
15. Kazenwadel, J., Secker, G. A., Betterman, K. L., and Harvey, N. L. (2012) *In vitro* assays using primary embryonic mouse lymphatic endothelial cells uncover key roles for FGFR1 signalling in lymphangiogenesis. *PLoS One* **7**, e40497
16. Murakami, M., and Simons, M. (2008) Fibroblast growth factor regulation of neovascularization. *Curr. Opin. Hematol.* **15**, 215–220
17. Shin, J. W., Min, M., Larrieu-Lahargue, F., Canron, X., Kunstfeld, R., Nguyen, L., Henderson, J. E., Bikfalvi, A., Detmar, M., and Hong, Y. K. (2006) Prox1 promotes lineage-specific expression of fibroblast growth factor (FGF) receptor-3 in lymphatic endothelium: A role for FGF signaling in lymphangiogenesis. *Mol. Biol. Cell* **17**, 576–584
18. Choi, I., Lee, S., Kyoung Chung, H., Suk Lee, Y., Eui Kim, K., Choi, D., Park, E. K., Yang, D., Ecoiffier, T., Monahan, J., Chen, W., Aguilar, B., Lee, H. N., Yoo, J., Koh, C. J., *et al.* (2012) 9-Cis retinoic acid promotes lymphangiogenesis and enhances lymphatic vessel regeneration: Therapeutic implications of 9-cis retinoic acid for secondary lymphedema. *Circulation* **125**, 872–882
19. Perrault, D. P., Lee, G. K., Park, S. Y., Lee, S., Choi, D., Jung, E., Seong, Y. J., Park, E. K., Sung, C., Yu, R., Bouz, A., Pourmoussa, A., Kim, S. J., Hong, Y. K., and Wong, A. K. (2019) Small peptide modulation of fibroblast growth factor receptor 3-dependent postnatal lymphangiogenesis. *Lymphat. Res. Biol.* **17**, 19–29
20. Yu, P., Wilhelm, K., Dubrac, A., Tung, J. K., Alves, T. C., Fang, J. S., Xie, Y., Zhu, J., Chen, Z., De Smet, F., Zhang, J., Jin, S. W., Sun, L., Sun, H., Kibbey, R. G., *et al.* (2017) FGF-dependent metabolic control of vascular development. *Nature* **545**, 224–228
21. Lee, H. W., Yu, P., and Simons, M. (2018) Recent advances in understanding lymphangiogenesis and metabolism. *F1000Res.* **7**. F1000 Faculty Rev-1114
22. Wong, B. W., Zecchin, A., Garcia-Caballero, M., and Carmeliet, P. (2018) Emerging concepts in organ-specific lymphatic vessels and metabolic regulation of lymphatic development. *Dev. Cell* **45**, 289–301
23. Yu, P., Wu, G., Lee, H. W., and Simons, M. (2018) Endothelial metabolic control of lymphangiogenesis. *Bioessays* **40**, e1700245
24. Teuwen, L. A., Geldhof, V., and Carmeliet, P. (2019) How glucose, glutamine and fatty acid metabolism shape blood and lymph vessel development. *Dev. Biol.* **447**, 90–102
25. Ma, W., Gil, H. J., Liu, X., Diebold, L. P., Morgan, M. A., Oxendine-Burns, M. J., Gao, P., Chandel, N. S., and Oliver, G. (2021) Mitochondrial respiration controls the Prox1-Vegfr3 feedback loop during lymphatic endothelial cell fate specification and maintenance. *Sci. Adv.* **7**, eabe7359
26. De Bock, K., Georgiadou, M., Schoors, S., Kuchnio, A., Wong, B. W., Cantelmo, A. R., Quaegebeur, A., Ghesquiere, B., Cauwenberghs, S., Eelen, G., Phng, L. K., Betz, I., Tembuyser, B., Brepoels, K., Welti, J., *et al.* (2013) Role of PFKFB3-driven glycolysis in vessel sprouting. *Cell* **154**, 651–663
27. Wong, B. W., Wang, X., Zecchin, A., Thienpont, B., Cornelissen, I., Kalucka, J., Garcia-Caballero, M., Missiaen, R., Huang, H., Bruning, U., Blacher, S., Vinckier, S., Goveia, J., Knobloch, M., Zhao, H., *et al.* (2017) The role of fatty acid beta-oxidation in lymphangiogenesis. *Nature* **542**, 49–54
28. Schoors, S., Bruning, U., Missiaen, R., Queiroz, K. C., Borgers, G., Elia, I., Zecchin, A., Cantelmo, A. R., Christen, S., Goveia, J., Heggermont, W., Godde, L., Vinckier, S., Van Veldhoven, P. P., Eelen, G., *et al.* (2015) Fatty acid carbon is essential for dNTP synthesis in endothelial cells. *Nature* **520**, 192–197
29. Huang, H., Vandekeere, S., Kalucka, J., Bierhansl, L., Zecchin, A., Bruning, U., Visnagri, A., Yuldasheva, N., Goveia, J., Cruys, B., Brepoels, K., Wyns, S., Rayport, S., Ghesquiere, B., Vinckier, S., *et al.* (2017) Role of glutamine and interlinked asparagine metabolism in vessel formation. *EMBO J.* **36**, 2334–2352
30. Kim, B., Li, J., Jang, C., and Arany, Z. (2017) Glutamine fuels proliferation but not migration of endothelial cells. *EMBO J.* **36**, 2321–2333
31. Futami, T., Okada, H., Kihara, R., Kawase, T., Nakayama, A., Suzuki, T., Kameda, M., Shindoh, N., Terasaka, T., Hirano, M., and Kuromitsu, S. (2017) ASP5878, a novel inhibitor of FGFR1, 2, 3, and 4, inhibits the growth of FGF19-expressing hepatocellular carcinoma. *Mol. Cancer Ther.* **16**, 68–75
32. Kikuchi, A., Suzuki, T., Nakazawa, T., Iizuka, M., Nakayama, A., Ozawa, T., Kameda, M., Shindoh, N., Terasaka, T., Hirano, M., and Kuromitsu, S. (2017) ASP5878, a selective FGFR inhibitor, to treat FGFR3-dependent urothelial cancer with or without chemoresistance. *Cancer Sci.* **108**, 236–242
33. Ornitz, D. M., and Itoh, N. (2015) The fibroblast growth factor signaling pathway. *Wiley Interdiscip. Rev. Dev. Biol.* **4**, 215–266
34. Murakami, M., Nguyen, L. T., Hatanaka, K., Schachterle, W., Chen, P. Y., Zhuang, Z. W., Black, B. L., and Simons, M. (2011) FGF-dependent regulation of VEGF receptor 2 expression in mice. *J. Clin. Invest.* **121**, 2668–2678
35. Ichise, T., Yoshida, N., and Ichise, H. (2014) FGF2-induced Ras-MAPK signalling maintains lymphatic endothelial cell identity by upregulating endothelial-cell-specific gene expression and suppressing TGFbeta signalling through Smad2. *J. Cell Sci.* **127**, 845–857
36. Deng, Y., Atri, D., Eichmann, A., and Simons, M. (2013) Endothelial ERK signaling controls lymphatic fate specification. *J. Clin. Invest.* **123**, 1202–1215
37. Deng, Y., Larrivee, B., Zhuang, Z. W., Atri, D., Moraes, F., Prahst, C., Eichmann, A., and Simons, M. (2013) Endothelial RAF1/ERK activation regulates arterial morphogenesis. *Blood* **121**, 3988–3996. S1-9
38. Ahmadian, M., Suh, J. M., Hah, N., Liddle, C., Atkins, A. R., Downes, M., and Evans, R. M. (2013) PPARgamma signaling and metabolism: The good, the bad and the future. *Nat. Med.* **19**, 557–566
39. Song, S., Attia, R. R., Connaughton, S., Niesen, M. I., Ness, G. C., Elam, M. B., Hori, R. T., Cook, G. A., and Park, E. A. (2010) Peroxisome proliferator activated receptor alpha (PPARalpha) and PPAR gamma coactivator (PGC-1alpha) induce carnitine palmitoyltransferase IA (CPT-1A) via independent gene elements. *Mol. Cell. Endocrinol.* **325**, 54–63
40. Sharma, S., Sun, X., Rafikov, R., Kumar, S., Hou, Y., Oishi, P. E., Datar, S. A., Raff, G., Fineman, J. R., and Black, S. M. (2012) PPAR-gamma regulates carnitine homeostasis and mitochondrial function in a lamb model of increased pulmonary blood flow. *PLoS One* **7**, e41555
41. Xu, H. E., Stanley, T. B., Montana, V. G., Lambert, M. H., Shearer, B. G., Cobb, J. E., McKee, D. D., Galardi, C. M., Plunket, K. D., Nolte, R. T.,

Parks, D. J., Moore, J. T., Kliewer, S. A., Willson, T. M., and Stimmel, J. B. (2002) Structural basis for antagonist-mediated recruitment of nuclear co-repressors by PPARalpha. *Nature* **415**, 813–817

42. Michelet, X., Dyck, L., Hogan, A., Loftus, R. M., Duquette, D., Wei, K., Beyaz, S., Tavakkoli, A., Foley, C., Donnelly, R., O'Farrelly, C., Raverdeau, M., Vernon, A., Pettee, W., O'Shea, D., *et al.* (2018) Metabolic reprogramming of natural killer cells in obesity limits antitumor responses. *Nat. Immunol.* **19**, 1330–1340
43. Leesnitzer, L. M., Parks, D. J., Bledsoe, R. K., Cobb, J. E., Collins, J. L., Consler, T. G., Davis, R. G., Hull-Ryde, E. A., Lenhard, J. M., Patel, L., Plunket, K. D., Shenk, J. L., Stimmel, J. B., Therapontos, C., Willson, T. M., *et al.* (2002) Functional consequences of cysteine modification in the ligand binding sites of peroxisome proliferator activated receptors by GW9662. *Biochemistry* **41**, 6640–6650
44. Guo, B., Huang, X., Lee, M. R., Lee, S. A., and Broxmeyer, H. E. (2018) Antagonism of PPAR-gamma signaling expands human hematopoietic stem and progenitor cells by enhancing glycolysis. *Nat. Med.* **24**, 360–367
45. Garcia, D., and Shaw, R. J. (2017) AMPK: Mechanisms of cellular energy sensing and restoration of metabolic balance. *Mol. Cell* **66**, 789–800
46. Wang, Q., Liang, B., Shirwany, N. A., and Zou, M. H. (2011) 2-Deoxy-D-glucose treatment of endothelial cells induces autophagy by reactive oxygen species-mediated activation of the AMP-activated protein kinase. *PLoS One* **6**, e17234
47. Kalucka, J., Bierhansl, L., Conchinha, N. V., Missiaen, R., Elia, I., Bruning, U., Scheinok, S., Treps, L., Cantelmo, A. R., Dubois, C., de Zeeuw, P., Goveia, J., Zecchin, A., Taverna, F., Morales-Rodriguez, F., *et al.* (2018) Quiescent endothelial cells upregulate fatty acid beta-oxidation for vasculoprotection via redox homeostasis. *Cell Metab.* **28**, 881–894.e813
48. Aloia, A., Mullhaupt, D., Chabbert, C. D., Eberhart, T., Fluckiger-Mangual, S., Vukolic, A., Eichhoff, O., Irmisch, A., Alexander, L. T., Scibona, E., Frederick, D. T., Miao, B., Tian, T., Cheng, C., Kwong, L. N., *et al.* (2019) A fatty acid oxidation-dependent metabolic shift regulates the adaptation of BRAF-mutated melanoma to MAPK inhibitors. *Clin. Cancer Res.* **25**, 6852–6867
49. Jiao, P., Feng, B., Li, Y., He, Q., and Xu, H. (2013) Hepatic ERK activity plays a role in energy metabolism. *Mol. Cell. Endocrinol.* **375**, 157–166
50. Xiao, Y., Liu, H., Yu, J., Zhao, Z., Xiao, F., Xia, T., Wang, C., Li, K., Deng, J., Guo, Y., Chen, S., Chen, Y., and Guo, F. (2016) Activation of ERK1/2 ameliorates liver steatosis in leptin receptor-deficient (db/db) mice via stimulating ATG7-dependent autophagy. *Diabetes* **65**, 393–405
51. Touat, M., Ileana, E., Postel-Vinay, S., Andre, F., and Soria, J. C. (2015) Targeting FGFR signaling in cancer. *Clin. Cancer Res.* **21**, 2684–2694
52. Stacker, S. A., Williams, S. P., Karnezis, T., Shayan, R., Fox, S. B., and Achen, M. G. (2014) Lymphangiogenesis and lymphatic vessel remodelling in cancer. *Nat. Rev. Cancer* **14**, 159–172
53. Yu, P., Alves, T. C., Kibbey, R. G., and Simons, M. (2018) Metabolic analysis of lymphatic endothelial cells. *Methods Mol. Biol.* **1846**, 325–334
54. Aas, V., Rokling-Andersen, M. H., Kase, E. T., Thoresen, G. H., and Rustan, A. C. (2006) Eicosapentaenoic acid (20:5 n-3) increases fatty acid and glucose uptake in cultured human skeletal muscle cells. *J. Lipid Res.* **47**, 366–374